Gazi University Journal of Science
GU J Sci
25(2):505-517 (2012)

ORIGINAL ARTICLE

The Prediction of Heat Transfer and Fluid Characteristics for Equilateral Triangular Bodies in Tandem Arrangement by Artificial Neural Networks

Eyüphan MANAY[1♠], Sibel GÜNEŞ[2], Esra AKÇADIRCI[2], Veysel ÖZCEYHAN[2], Uğur ÇAKIR[1], Ömer ÇOMAKLI[1]

[1]*Department of Mechanical Engineering, Faculty of Engineering, Bayburt University, 69000, Bayburt, Turkey,*
[2,]*Department of Mechanical Engineering, Faculty of Engineering, Erciyes University, 38039, Kayseri, Turkey,*

Received:30/01/2011 Revised:08/03/2011 Accepted:30/01/2012

ABSTRACT

The objective of this study is to investigate the effect of the spacing between equilateral dual triangular bodies symmetrically placed into the channel axis under steady state conditions on heat transfer and fluid characteristics by using artificial neural networks (ANN). The Back Propagation (BP) training algorithm was applied to train the model. The successful application proved that ANN model can be used for predicting the Nusselt number and skin friction coefficient as a convenient and effective method. The distribution of local Nusselt number, skin friction coefficient along the channel wall and overall enhancement ratio of all investigated cases are presented.

Keywords: Heat transfer enhancement; tandem arrangement; triangular body; artificial neural network.

1. INTRODUCTION

Heat transfer enhancement technology has been extensively used in heat exchanger applications; such as automotives, refrigeration, process and chemical industry, etc. There exist various methods for enhancing heat transfer. Inserting different shaped elements in channel flow is one of the widely-used heat transfer enhancement technique [1-3]. Placing sharp edged bodies in a smooth channel is also an effective method for enhancing heat transfer concerning with the bodies interrupting the wall sublayer. This yields flow turbulence, separation and reattachment leading to higher heat transfer rates. The body placed in a smooth channel cause an increase in turbulent intensity and flow mixing, thus induce a recirculation zone or vortices flow behind the body. Although heat transfer is increased through the body arrangement, the pressure drop of the channel flow is also increased due to the decreased flow area effects. So, the geometric dimensions of the bodies, spacing between triangular bodies and arrangement type play important role on heat transfer and fluid characteristics.

The most commonly studied shapes include cylinders of circular and square cross-sections. The effects of the Reynolds and Prandtl numbers on the rate of heat transfer from a square cylinder were investigated numerically in the two-dimensional unsteady periodic flow regime, in the range of conditions $60 \le \mathrm{Re} \le 160$ and $0.7 \le \mathrm{Pr} \le 50$ by Sahu [4]. Turki [5] numerically investigated the unsteady flow and heat transfer characteristics on a square cylinder placed horizontally into the channel. The results were presented in order to indicate the influence of the channel blockage ratio, Reynolds and Richardson numbers on the flow structure and the heat transfer originated from the square cylinder. Mixed convection in a symmetrically heated horizontal channel in which a square cylinder inserted was investigated numerically

♠Corresponding author, e-mail: emanay@bayburt.edu.tr

by Biswas [6] The results indicated that the thermal buoyancy could perturb the steady wake or attached vortices at the rear of the obstacle and induce transition to periodic flow.

In steady flow regime the heat transfer characteristics from a circular cylinder were studied detailed in the range of Prandtl number 0.7 to 400 [7]. Similarly, other researchers recently have studied in steady flow regime for two circular cylinders in tandem arrangement at four different Prandtl numbers 0.1, 1, 10 and 100 [8]. The effect of aspect ratio of a cylinder on heat transfer was studied experimentally in cross flow of air by Chang and Mills [9]. They reported that the heat transfer rates increased with decreasing aspect ratio at the center plane on the rear of the cylinder. Consequently, the average Nusselt number correlations were presented that account for the effects of aspect ratio, tunnel blockage and free stream turbulence.

Flow over bluff bodies is a considerable subject for many engineering applications, such as flows around buildings, bridges, marine risers and in the context of heat transfer enhancement. The flow over bodies in tandem arrangement may include complex interactions between the shear layers, vortices and Karman vortex streets [10]. Researchers numerically studied the laminar convective heat transfer from dual isothermal cylinders in tandem arrangement for unsteady flow regime. The mean and local Nusselt numbers for the upstream and downstream cylinders were obtained. They concluded that the mean Nusselt number of the upstream cylinder came close to that of a single isothermal cylinder for L/D > 4, and, the mean Nusselt number of the downstream cylinder was approximately 80% of the upstream cylinder [11]. The flows over square cylinders in tandem arrangement were investigated both numerically and experimentally. The effect of spacing ratio between the bodies on heat transfer and flow characteristics were analyzed [12-13].

The literature survey shows that flow around bluff bodies such as cylinder and square cylinder has been studied extensively in detail due to their practical relevance. However, triangular bodies have been rarely studied by some researchers, moreover there is no investigation available in literature concerning with the tandem arrangement of triangular bodies [14-15]. Artificial neural network (ANN) has been increasingly preferred by researchers in order to avoid the use of a time-consuming and iterative solution. So, ANN has been commonly used in various engineering application areas such as heating, ventilating, air conditioning and power generation systems, solar steam generators and refrigeration etc [16].

The fundamental objective of this study is both to investigate the effect of the spacing between equilateral triangular bodies on heat transfer and fluid characteristics and to show the applicability of artificial neural network (ANN) for predicting Nusselt number and skin friction coefficient in a horizontal channel in which dual triangular bodies placed in tandem arrangement in Reynolds number range varying from 10.000 to 40.000 by both CFD and ANN.

2. CFD ANALYSIS

2.1. Problem description

A schematic view of the computational domain is presented in Figure 1 (a) where the equilateral triangular bodies are placed in tandem arrangement. The numerical simulations have been conducted in two-dimensional domain, which represents a channel height (H) of 4B and channel length (L) of 36B. B is the edge length of the equilateral triangular bodies and W is the spacing between the bodies. While the channel length was 36B, the location of the first triangular body (S) was maintained at x = 8B. The length of the inlet section was selected long enough to provide a fully developed flow, and also the length of the outlet section was selected long enough to prevent the adverse pressure effects at the exit. For getting idea about where the local Nusselt number and skin friction coefficient values were determined, the calculating section was presented in Figure 2. Four different W/B ratios were considered as 2, 3, 4 and 5 [17-18].

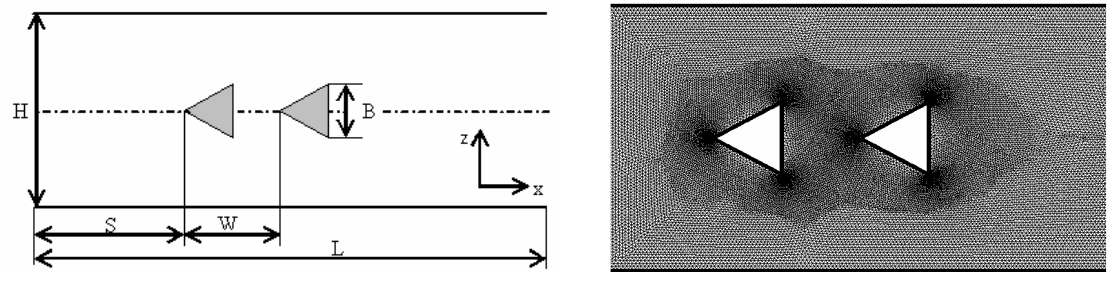

(a) (b)

Figure 1. (a) Computational domain and the triangular bodies in tandem arrangement, (b) part of numerical mesh.

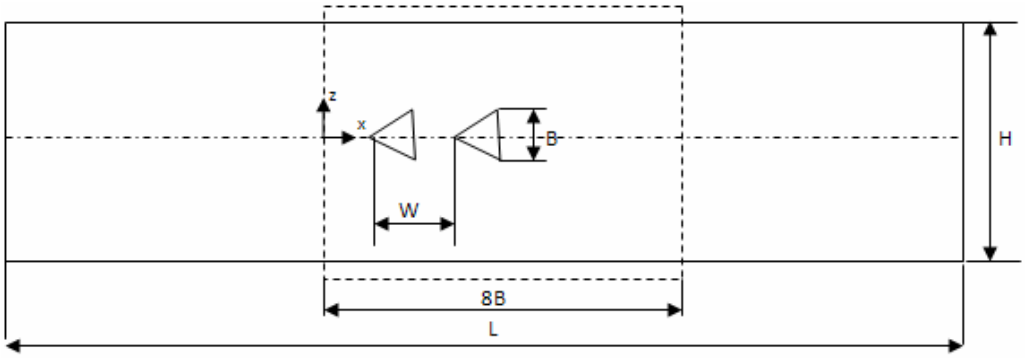

Figure 2. Calculating section of local Nusselt number and skin friction coefficient.

The computational domain consisting of a grid structure with approximately 1894664 cells, is shown in Figure 1 (b). The mesh is highly concentrated near the wall boundaries of the triangular bodies and also in the regions near the channel walls. The cell number is varied from 1368494 to 2265316 various steps for grid independence test. It was seen that after 1894664 cells, there was no significant increase in Nusselt number which is taken as criterion for grid independence.

2.2 Numerical procedure

CFD calculations are performed to solve the problem depending on the numerical model, boundary conditions, assumptions, and numerical values in order to determine the temperature and velocity distributions in the flow field. Segregated manner was selected as solver type, due to its advantage of strong coupling between the velocity and pressure. This advantage helps to prevent from convergence problems and oscillations in pressure and velocity fields. (SST) k- ω turbulence model is allowed to predict the heat transfer and fluid flow characteristics by using the computational fluid dynamics (CFD) commercial code of Fluent [19]. The first order upwind numerical scheme and SIMPLE (semi-implicit method for pressure linked equations) algorithm are utilized to discretize the governing equations. This algorithm is more stable and economical in comparison with the other algorithms. The solutions were considered to converge when the normalized residual values were 10^{-7} for the energy and 10^{-4} for the other variables. It is assumed that the problem is described by the two-dimensional, steady continuity, momentum and energy equations with constant thermophysical properties.

Continuity equation:

$$\frac{\partial u}{\partial x}+\frac{\partial v}{\partial y}=0 \qquad (1)$$

Momentum equation:

$$u\frac{\partial u}{\partial x}+v\frac{\partial u}{\partial y}=-\frac{1}{\rho}\frac{\partial P}{\partial x}+\nu\left(\frac{\partial^2 u}{\partial x^2}+\frac{\partial^2 u}{\partial y^2}\right) \qquad (2)$$

$$u\frac{\partial v}{\partial x}+v\frac{\partial v}{\partial y}=-\frac{1}{\rho}\frac{\partial P}{\partial y}+\nu\left(\frac{\partial^2 v}{\partial x^2}+\frac{\partial^2 v}{\partial y^2}\right) \qquad (3)$$

Energy equation:

$$u\frac{\partial T}{\partial x}+v\frac{\partial T}{\partial y}=\alpha\left(\frac{\partial^2 T}{\partial x^2}+\frac{\partial^2 T}{\partial y^2}\right) \qquad (4)$$

and k_{eff} is the effective conductivity. Researchers developed the shear-stress transport (SST) k– ω model by blending k– ω model and k-ε model formulation effectively [20]. In literature, there exist various numerical studies concerning with channel flow which are performed by using (SST) k- ω turbulence model. Heat transfer enhancement in the channels equipped with baffle inserts has been widely investigated numerically, and, it was concluded that (SST) k- ω predicted successfully and accurately the flow modification [21-25]. The (SST) k- ω model is able to calculate speedly two-dimensional flow and also predict the interactions with the wall. This model is also advantageous because the model equations behave compatible in both the near-wall and far-field regions.

In the derivation of the k–ω model, the flow is assumed to be fully turbulent. The Shear-Stress Transport (SST) k-ω model, the turbulence kinetic energy, k, and the specific dissipation rate, ω, are obtained from the following transport equations:

$$\frac{\partial}{\partial t}(\rho \mathrm{k})+\frac{\partial}{\partial x_i}\left(\rho k u_i\right)=\frac{\partial}{\partial x_j}\left(\Gamma_k\frac{\partial k}{\partial x_j}\right)+G_k-Y_k \qquad (5)$$

and

$$\frac{\partial}{\partial t}(\rho\omega)+\frac{\partial}{\partial x_i}\left(\rho\omega u_i\right)=\frac{\partial}{\partial x_j}\left(\Gamma_\omega\frac{\partial \omega}{\partial x_j}\right)+G_\omega-Y_\omega+D_\omega \qquad (6)$$

In these equations, G_k represents the generation of turbulence kinetic energy due to mean velocity gradients. G_ω represents the generation of ω. Γ_k and Γ_ω represent the effective diffusivity of k and ω, respectively. Y_k and Y_ω represent the dissipation of k and ω due to turbulence and D_ω represents the cross-diffusion term. The calculation of all of the above terms

is given detailed in reference [19]. Two parameters of interest for this study are the skin friction coefficient and the Nusselt number. The skin friction coefficient *Cf* is defined by

$$C_f = \frac{\tau_s}{\frac{1}{2}\rho U_m^2} \tag{7}$$

The heat transfer performance is evalauted by Nusselt number which can be obtained by the local temperature gradient as:

$$Nu_x = -\frac{\partial T}{\partial Z} \tag{8}$$

The average Nusselt number can be calculated as follows:

$$Nu_{av} = \int Nu_x \frac{\partial x}{L} \tag{9}$$

where L is the length of computational domain. The friction factor is determined from;

$$f = \frac{\Delta P}{\frac{1}{2}\rho U_m{}^2 \frac{L}{H}} \tag{10}$$

in which pressure ΔP is pressure difference between the channel inlet and outlet.

2.3 Boundary conditions

The solution domain of the considered 2D channel flow is geometrically quite simple, which is a rectangle on the *x–z* plane, enclosed by the inlet, outlet and wall boundaries. The working fluid in all cases is water. The inlet temperature of water was considered to be uniform at 300 K. The thermophysical data of the fluid at 300 K is given in Table 1.On walls, no-slip conditions were used for the momentum equations. A constant surface temperature of 350 K was applied to the bottom wall of the channel. The upper wall and the triangular bodies were assumed to be adiabatic. Uniform velocity was imposed to inlet plane and the Reynolds number varies from 10.000 to 40.000. The outlet boundary condition was natural condition which implies zero-gradient conditions at the outlet.

Table 1. The thermophysical data of the water at 300 K

T (K)	ρ **(kg/m^3)**	c_p **(kJ/kg K)**	$\mu.10^{-6}$ **(Ns/m^2)**	$\nu.10^{-6}$ **(m^2/s)**	k **(W/m K)**	$\alpha.10^{-6}$ **(m^2/s)**
300	996.05	4.0716	830	0.833	0.615	0.1517

3. ARTIFICIAL NEURAL NETWORKS

ANN is a computational model, which simulates the function of biological network, consisting of neurons. The system has three layers of neurons: input layer, a hidden layer and an output layer. The neurons of the network are attached to each other by the weights. Input layer includes all of the input factors; information is then processed through the hidden layer from the input layer and the following output vector is computed in the output layer. Figure 3 illustrates how information is processed through a single neuron which receives weighted activation from other neurons through its coming connections. First, these are added (summation function), and then the result passes through an activation function, and the output turns out to be the activation of the neuron. This activation value is multiplied with a specific weight and is transferred to the next neuron for each of the outgoing connections.

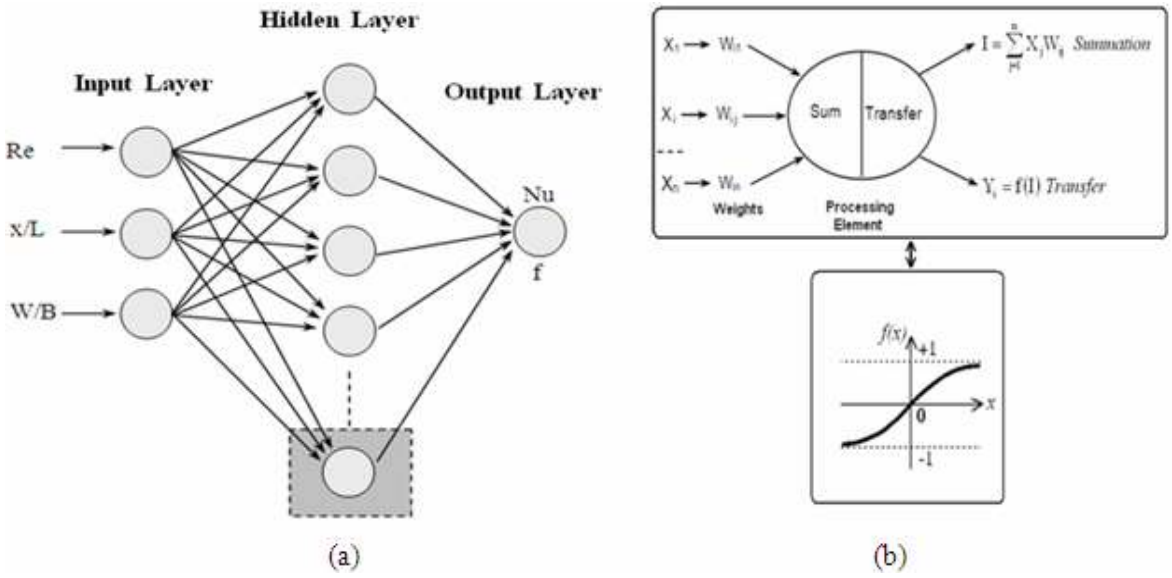

Figure 3. Architecture of an ANN model with one hidden layer; (a) artificial neural network, (b) information processing.

An ANN model is required to be trained from an available training set covering many pairs of input-output elements. The inputs of the network are Reynolds number, x/L and W/B ratios for each of training operation and the output is either Nusselt Number, skin friction coefficient or friction factor, respectively. In this study, the back-propagation learning algorithm was for one-hidden layer network. The tangent sigmoid transfer function

$$f(x)=\frac{2}{1+e^{-2x}}-1 \qquad (11)$$

Back Propagation is the most extensively preferred training algorithm for neural networks. The weights are updated as following:

$$\Delta w_{ij}(t)=-\eta\frac{\partial E(t)}{\partial w_{ij}(t)}+\alpha\Delta w_{ij}(t-1) \qquad (12)$$

Where η is the learning rate, and α is the momentum coefficient. In this study, a learning rate of 0.1 with momentum coefficient of 0.8 resulted in the fastest convergence. The configuration shown in Fig. 3 has 3-10-1 neurons in the input, hidden and output layers, respectively. The optimum number of neuron was determined by taking into account the performances of both training and test sets versus training iteration with various number of hidden neurons. If the hidden layer contains too few neurons, the network may not be capable of learning correctly and the output of the network to test data would be insufficient. Conversely, if the hidden layer contains too many neurons, the solution surface created by the network may bring out wrong characteristics at points between training data. Ten hidden neurons were chosen to be most effective design.

In this study there are four data sets for the Reynolds number (10.000, 20.000, 30.000 and 40.000) and one data set for x/L for four different W/B ratios. One of the data set of Re=20.000 for W/B=3 obtained from CFD was used for test and rest of them are used for training. The Nusselt number, skin friction coefficient and friction coefficient were predicted by ANN for Re=15.000, 25.000 and 35.000 for all W/B ratios. The network was trained up to 100,000 training iterations for prediction of Nusselt number and skin friction coefficient.

Firstly, the connection weights are adjusted through input layer, hidden layer and output layer until the network model gives outputs that are close enough to the desired outputs for training procedure. Figure 4 shows the test results for predicting the Nusselt Number and skin friction coefficient. As observed from this figure, the CFD and ANN results are very close to each other. The deviations found for Nusselt number and skin friction factor were within ±3.6%, and ±7%, respectively.

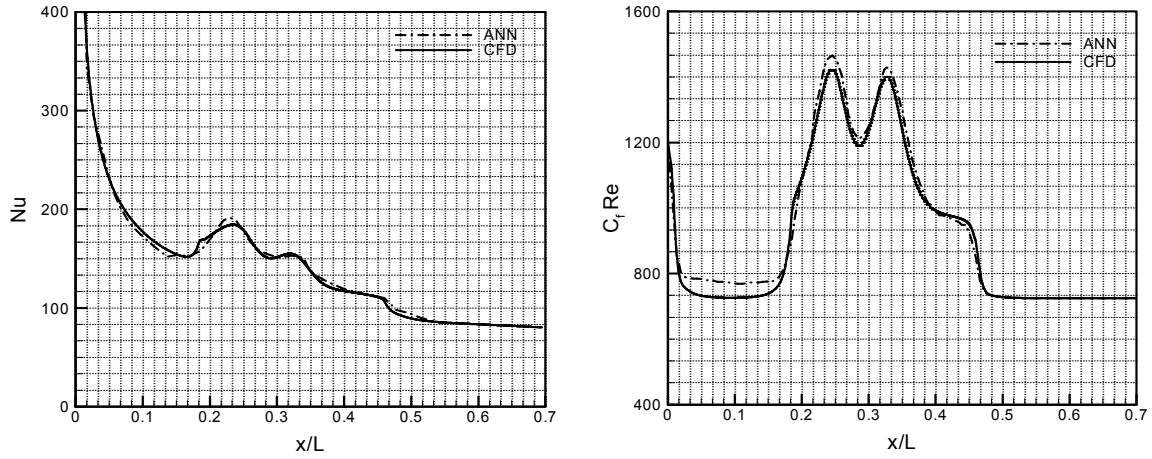

Figure 4. The comparison of predicted values (ANN) with calculated values (CFD) for W/B=3 and Re=20000.

4. RESULTS

In this work, the used numerical method to obtain results was validated with the study of Chattopadhyay [15] in which the augmentation of heat transfer in a channel with a single triangular prism was investigated. The results of Nusselt number and skin friction coefficient obtained from CFD analyses were compared with the results obtained from the study of Chattopadhyay [15]. Figure 5(a) reveals that the heat transfer results of the present study agree well with Chattopadhyay [15] with the deviations within ±7.8% for x/L values below 0.3. Figure 5(b) presents the skin friction factor results for smooth tube. As seen, the skin friction factor values of the present study are in good agreement with the results of Chattopadhyay [15] with the deviations within ±13% for x/L values below 0.3.

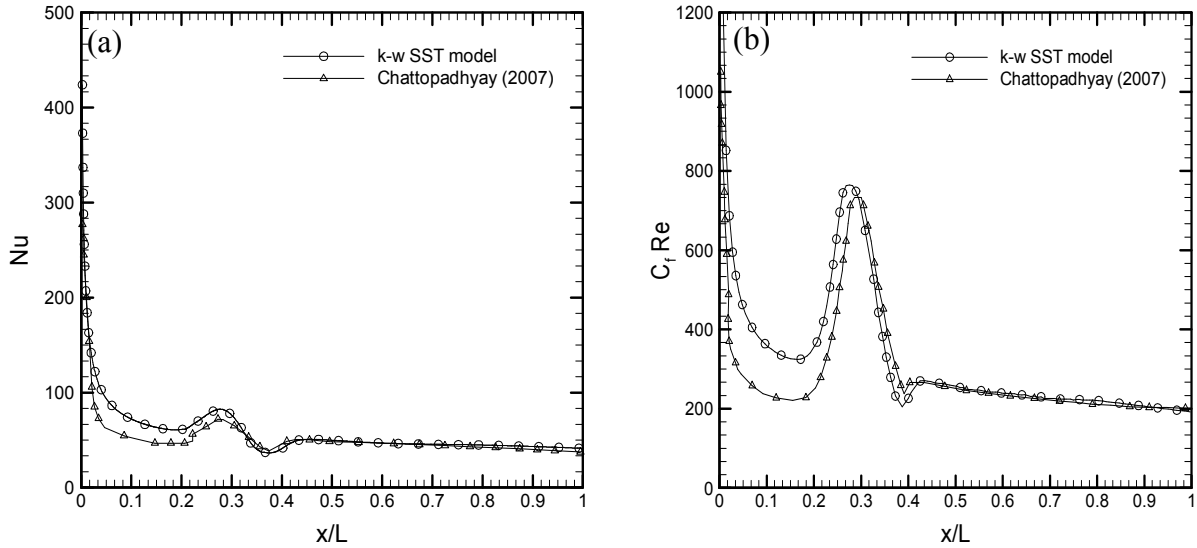

Figure 5. The comparison of the results of CFD and Chattopadhyay [15] for Re=20.000; (a) local Nusselt Number, (b) local skin friction coefficient.

In Figure 6, temperature contours of all cases studied numerically are presented for W/B=2, 3, 4 and 5. It can be clearly seen that the thermal boundary layer thickness decreases with the increase of Reynolds number from 10.000 to 40.000. Nearly, no change in the thickness of the thermal boundary layer is observed by the increase of gap ratio between the triangles. Figure 7 represents the distributions of velocity vectors. Velocity vectors have uniform distribution at the inlet of the test section. At W/B=2, because the gap length is very small, no reattachment is observed at the back track region of the first triangle. But, by the increase of the gap length (W/B=3) some vectors can reattach to the upstream and downstream. When the distributions and the directions of the vectors are examined at W/B=4 and especially 5, it can be said that the triangles treat as two separate bodies.

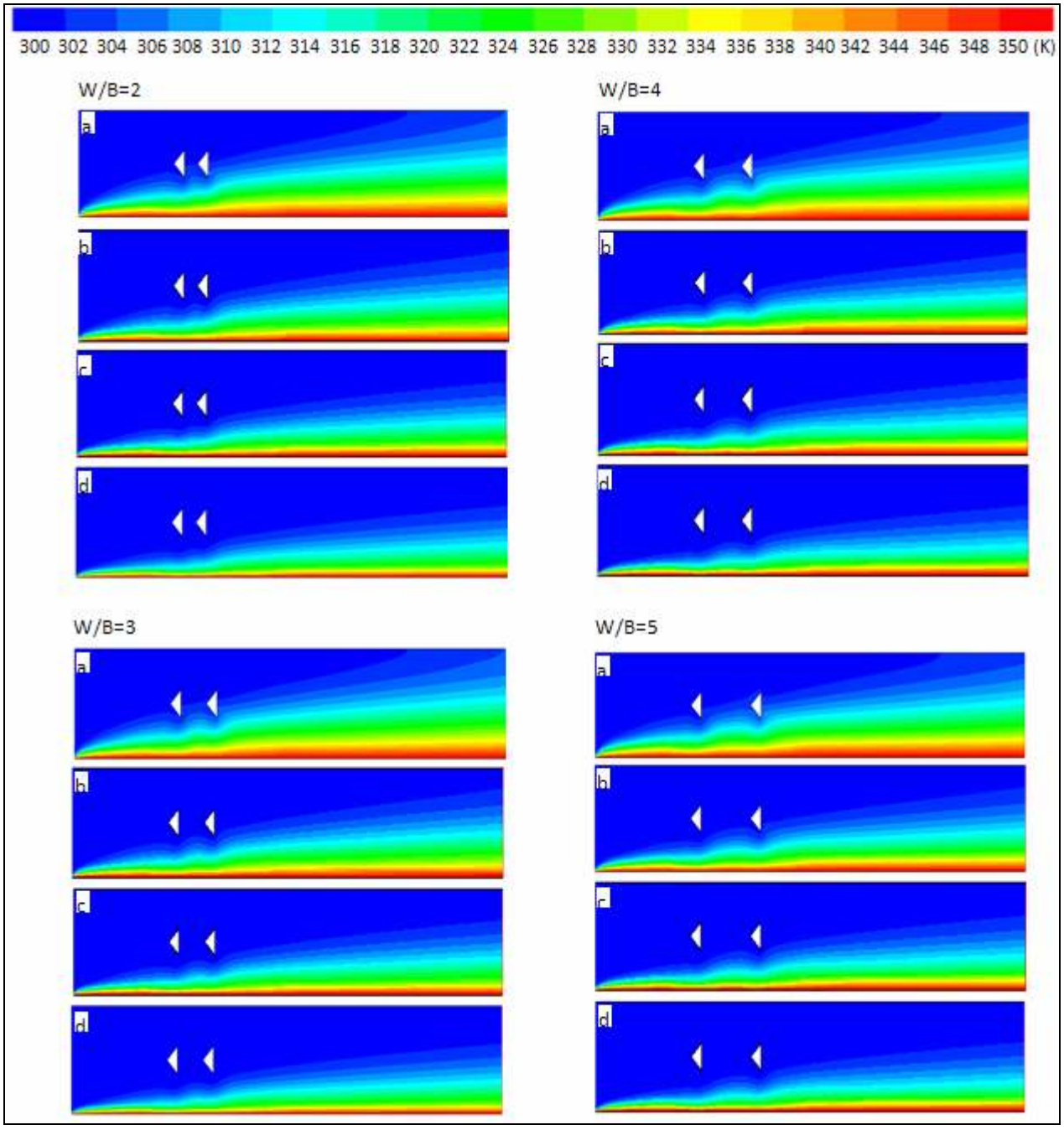

Figure 6. Temperature contours; (a) Re=10.000, (b) Re=20.000, (c) Re=30.000 and (d) Re=40.000.

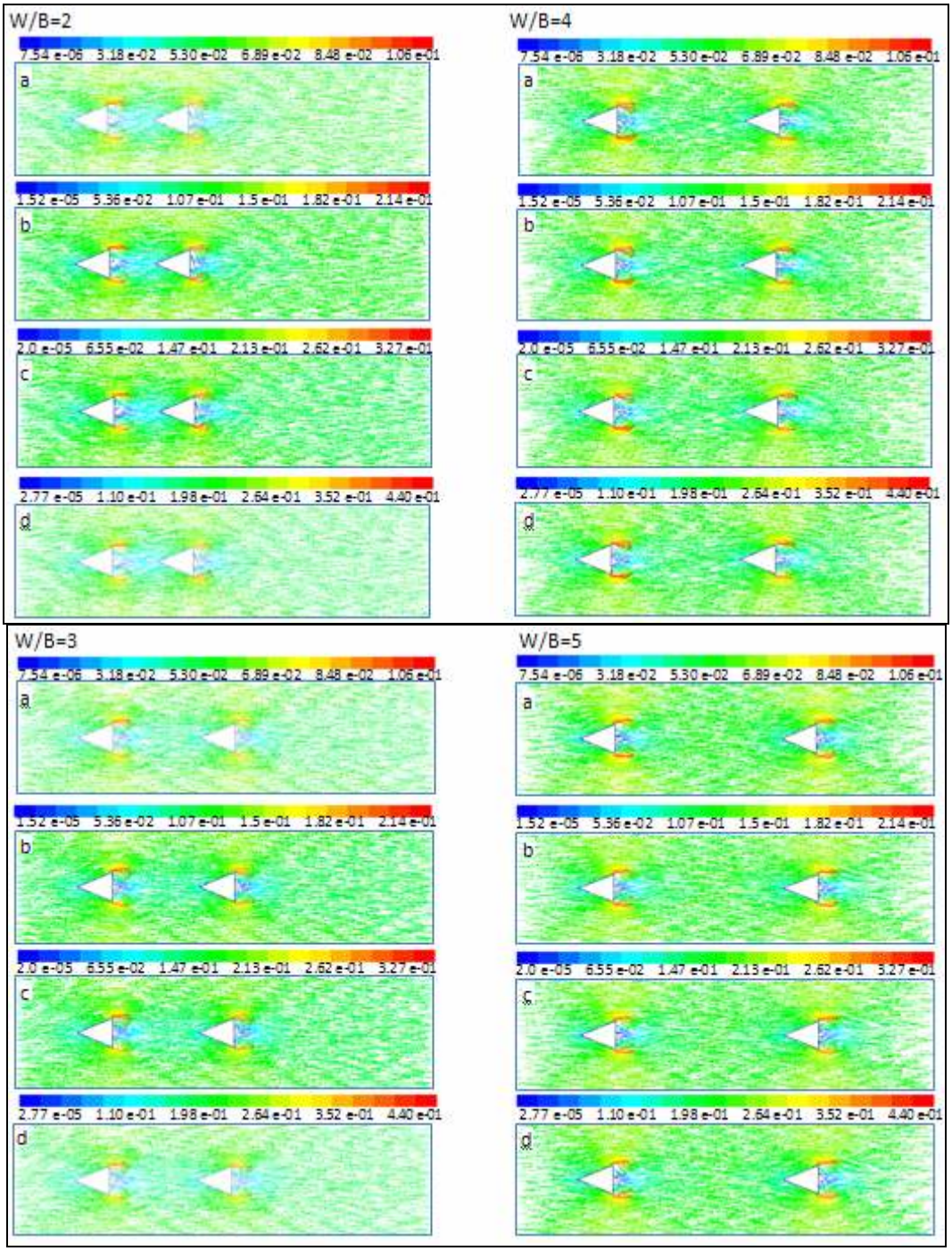

Figure 7. Velocity vectors; (a) Re=10.000, (b) Re=20.000, (c) Re=30.000 and (d) Re=40.000.

The distribution of local Nusselt number along the channel length is shown for tandem triangular bodies for different W/B ratios is illustrated in Fig. 8. The local Nusselt number takes a local maximum at the placed position of the upstream body, and at the placed position of the downstream body, after the second body a small crest can be observed due to the effect of vortex generation. On the other hand, after this small crest towards to the exit the Nusselt number decreases strongly due to the fact that the effect of the periodically shedding vortices do not occur from the bodies for all cases. Separated shear layer from downstream body and impinging of vortex formed by upstream body strongly increases heat transfer on downstream cylinder

.

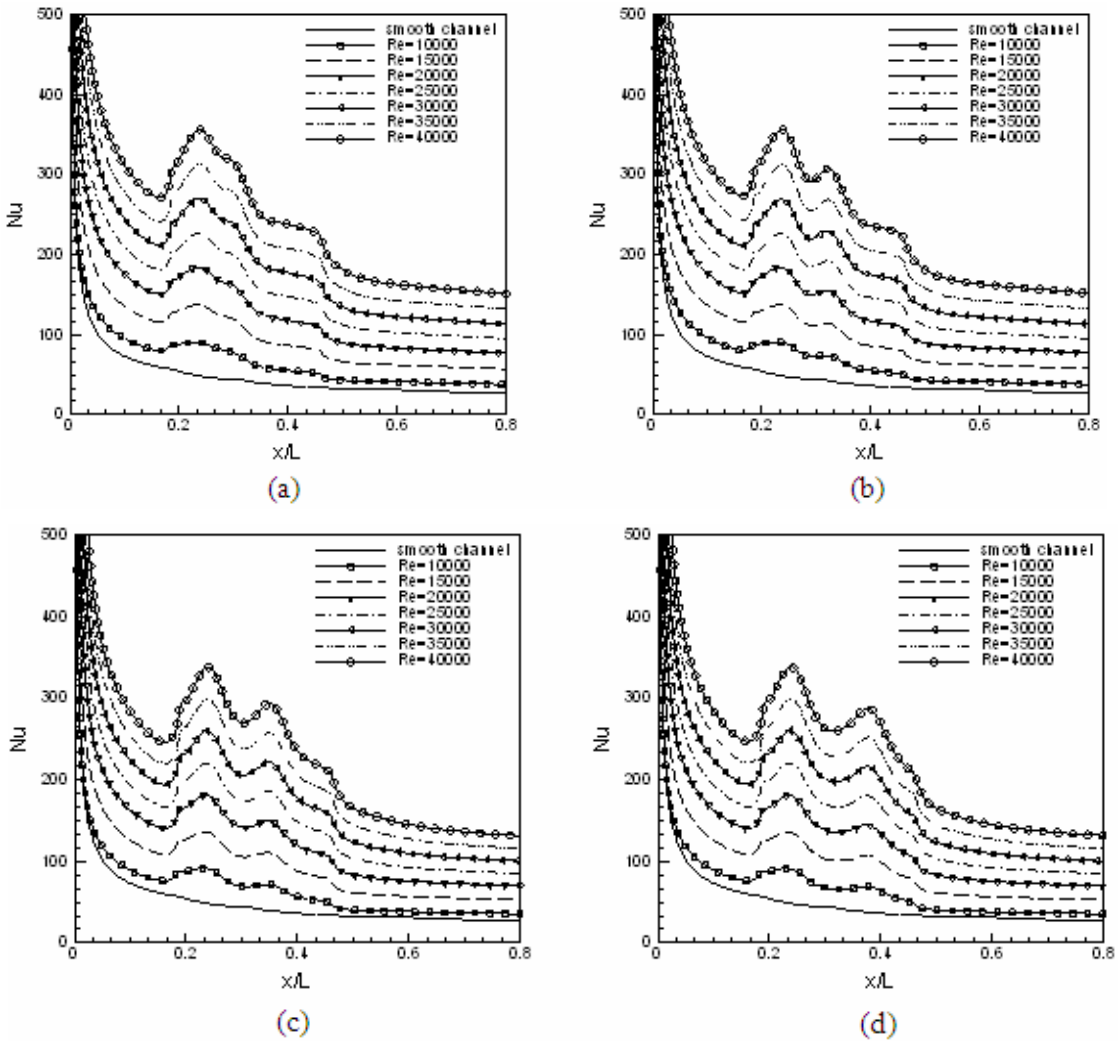

Figure 8. The distribution of local Nusselt number along the channel length for different W/B ratios (a) W/B=2, (b) W/B=3, (c) W/B=4, (d) W/B=5.

Nusselt number distribution for smooth channel, Re=10000 for all cases is also shown for comparison. As indicated in Figure 8(a), the local Nusselt number distribution trend for Re=10.000 looks like the trend in Figure 4(a), tandem bodies behave as a single body at Re=10.000 and 15.000 for the case of W/B=2. However, the peaks become obvious with increasing Reynolds number and W/B ratios. It can be discerned here that the patterns are similar for Fig.8(b)-(d). As expected local Nusselt number increases with increasing Reynolds number for all cases. The heat transfer enhances especially for upstream flow region concerning with the generation of vortices due to the first body as well as the role of turbulence in better mixing brings in the enhancement in heat transfer from the channel wall. The heat transfer improves as the interaction between the bodies increase that is to say the spacing between the bodies becomes closer.

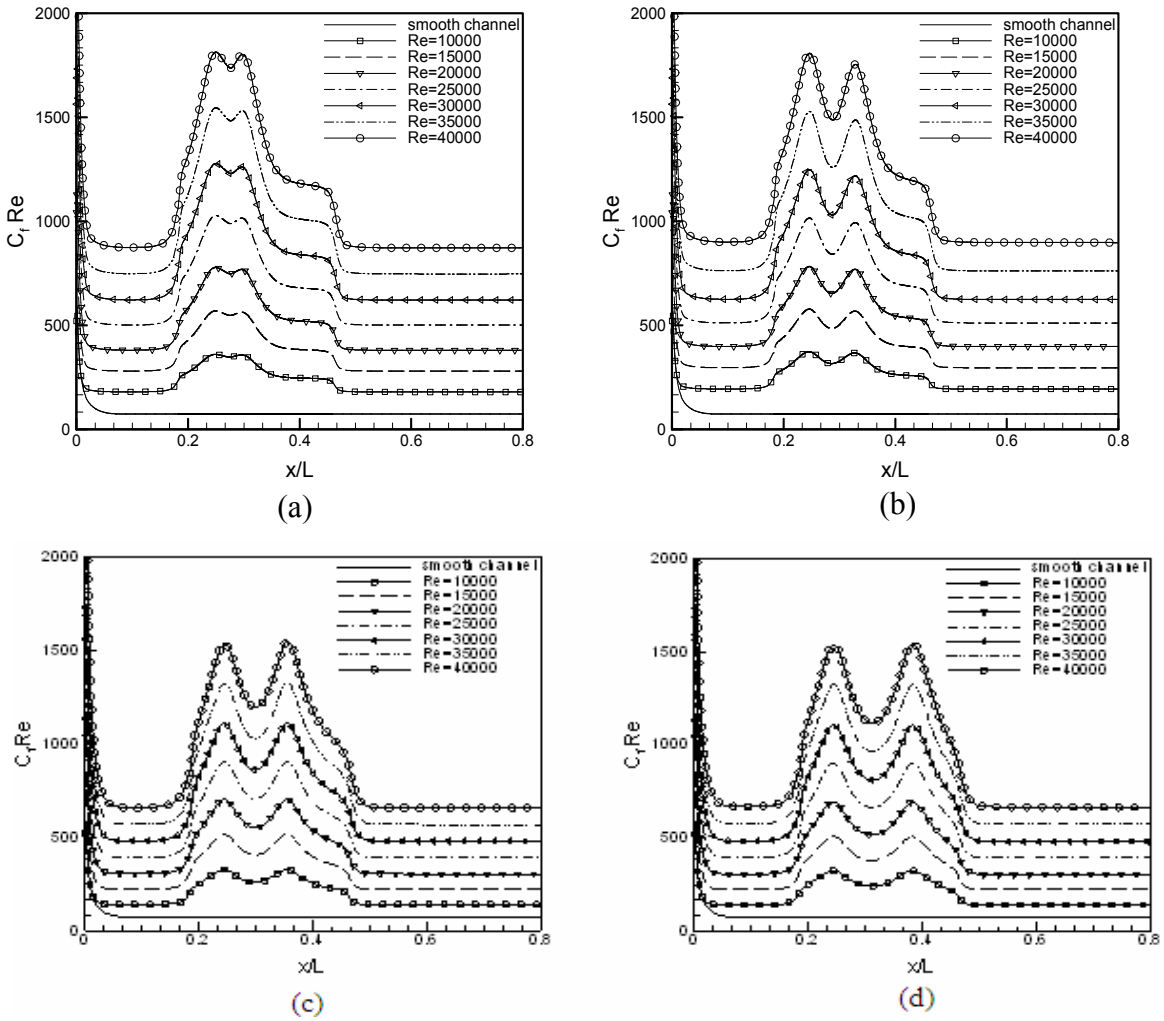

Figure 9. The distribution of local skin friction coefficient along the channel length for different W/B ratios (a) W/B=2, (b) W/B=3, (c) W/B=4, (d) W/B=5.

On the other hand, as expected, these bodies cause a significant fluid friction and pressure drop as well, in comparison with the smooth channel. The skin friction factor increases with decreasing spacing between the bodies due to the fact that interaction between the bodies disturb the entire flow field and cause more friction. The local skin friction coefficient distributions on the bottom channel wall are shown in Figure 9 for W/B=2, 3, 4 and 5, respectively. Similarly with local Nusselt number, the local skin friction coefficient takes a maximum both at the placed position of the first body and at the position of the downstream body in the tandem arrangements. In Figures 9(a)-9(d), the local distribution of the skin friction coefficient for smooth channel, Re=10.000 is also shown for comparison. The magnitude of skin friction is the highest at Re=40.000, for the case W/B=2 in which there is more flow resistance. It is evident from Figure 9(d) that the downstream flow becomes more regular when the bodies become distant from each other. The local skin friction coefficient increases with increasing Reynolds number for all cases.

Heat transfer enhancement is obtained at the expense of increased pressure drop caused by triangular bodies in tandem arrangement. Therefore, a performance analysis is required for the evaluation of the net energy gain to state if the method employed to increase the heat transfer is efficient or not. In this study, the overall performance is evaluated by the constant pumping power criterion. The overall enhancement ratios are determined from $(Nu_{tb}/Nu_s).(f_s/f_{tb})^{1/3}$ [26].

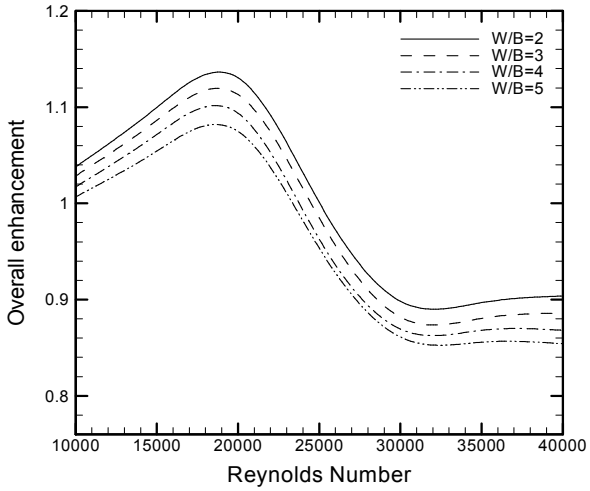

Figure 10. The overall enhancement ratio versus Reynolds number.

Figure 10 illustrates the overall enhancement ratio for all spacing ratios. The overall enhancement ratio increases up to approximately Re=19.000, and then decreases almost linearly to Re=30.000. After Re=30.000, the overall enhancement ratio does not change apparently for all cases. There will be a net energy gain if overall enhancement ratio is over one. So, it is evident from Fig. 10 that for all cases the overall enhancement ratio is over one up to Re=25.000. So, placing triangular bodies in tandem arrangement is not thermodynamically advantageous when Reynolds number is above 25.000. Because, the fluid friction dominates the heat transfer. The overall enhancement ratio decreases with increasing spacing ratios between the bodies. As a result, the best overall enhancement ratio of 1.14 was achieved at Re=19.000 for the case of W/B=2.

5. Conclusions

The artificial neural network (ANN) model was successfully utilized to predict the the local Nusselt number, skin friction coefficient and friction factor in a channel with dual triangular bodies in tandem arrangement for various spacing ratios between the bodies. The trained neural network was tested with data that were not used for the training, and, the ANN predictions agree reasonably well with the data obtained by CFD simulations. The local Nusselt number and skin friction coefficient take a local maximum at the placed position of the upstream body, and at the placed position of the downstream body. The heat transfer enhances especially for upstream flow region concerning with the generation of vortices. The increase in local Nusselt number, results in an increase in pressure drop, and, the friction factor increases with decreasing spacing between the bodies due to the fact that the close interaction between the bodies disturbs the entire flow field and causes more friction. Consequently, the best overall enhancement ratio of 1.14 was achieved at Re=19.000 for the case of W/B=2.

Acknowledgments

Authors would like to thank for the financial support of the TUBITAK (The Scientific and Technological Research Council of Turkey) under the contract: 107M508.

Nomenclature

B	base of the triangular body
C_f	skin friction coefficient
f	friction factor
g	gravitational acceleration
H	height of the computational domain
k	kinetic energy
L	length of domain in x direction
Nu	Nusselt number
P	Pressure
Pr	Prandtl number
Re	Reynolds number
S	location of the triangular bodies
T	temperature
U_m	mean velocity component in x direction
v	fluid velocity
W/B	spacing ratio

Greek symbols

ρ	fluid density
τ	shear stress
ω	specific dissipation rate
μ	dynamic viscosity

Subscripts

m	mean
s	smooth channel
tb	triangular body

REFERENCES

[1] Eimsa-ard, S. and Promvonge P., "Experimental investigation of heat transfer and friction characteristics in a circular tube fitted with V-nozzle turbulators", ***International Communications in Heat and Mass Transfer***, 33, 591-600, (2006).

[2] Khaled, RA., "Heat transfer enhancement in hairy fin systems", ***Applied Thermal Engineering***, 27:250-257 (2007).

[3] Shoji, Y., Sato, K. and Oliver, D.R., "Heat transfer enhancement in round tube using wire coil influence of length and segmentation", ***Heat Transfer-Asian Research***, 32 (2): 99-107 (2003).

[4] Sahu, A.K., Chhabra, R.P. and Eswaran, V., "Effects of Reynolds and Prandtl numbers on heat transfer from a square cylinder in the unsteady flow regime", ***International Journal of Heat and Mass Transfer***, 52, 839–850 (2009).

[5] Turki, S., Abbassi, H. and Ben Nasrallah, S., "Two-dimensional laminar fluid flow and heat transfer in a channel with a built-in heated square cylinder", ***International Journal of Thermal Sciences,*** 42: 1105–1113 (2003).

[6] Biswas, G., Laschefski, H., Mitra, N. K. and Fiebig, M., "Numerical investigations of mixed convection heat transfer in a horizontal channel with a built-in square cylinder", ***Numerical Heat Transfer***, Part A, 18, 173-188, (1990).

[7] Bharti, R.P., Chhabra, R.P. and Eswaran, V., "A numerical study of the steady forced convection heat transfer from an unconfined circular cylinder", Heat Mass Transfer, 41, 824–833, (2005).

[8] 8 .Juncu, G., "A numerical study of momentum and forced convection heat transfer around two tandem circular cylinders at low Reynolds numbers", Part II Forced convection heat transfer, ***International Journal of Heat Mass Transfer,*** 50, 3799–3808, (2007).

[9] Chang, B.H. and Mills, A.F., "Effect of aspect ratio on forced convection heat transfer from cylinders", ***International Journal of Heat and Mass Transfer,*** 47:1289–1296 (2004).

[10] Bhattacharyya, S. and Dhinakaran, S., "Vortex shedding in shear flow past tandem square cylinders in the vicinity of a plane wall", ***Journal of Fluids and Structures,*** 24:400–417 (2008).

[11] Mahir, N. and Altaç, Z., "Numerical investigation of convective heat transfer in unsteady flow past two cylinders in tandem arrangements", ***International Journal of Heat and Fluid Flow***, 29:1309–1318, (2008).

[12] Tatsutani, R.K., Devarakonda, R. and Humphrey, J.A.C., "Unsteady flow and heat transfer for cylinder pairs in a channel", ***International Journal of Heat and Mass Transfer,*** 36:3311–3328 (1993).

[13] Rosales, J.L., Ortega, A. and Humphrey, J.A.C., "A numerical simulation of the convective heat transfer in confined channel flow past square cylinders: comparison of inline and offset tandem pairs", ***International Journal of Heat and Mass Transfer***, 44:587–603 (2001).

[14] Abbassi, H., Turki, S. and Ben Nasrallah, S., "Mixed convection in a plane channel with a built-in triangular prism", ***Numerical Heat Transfer, Part*** A, 39, 307-320 (2001).

[15] Chattopadhyay, H., "Augmentation of Heat Transfer in a Channel using Triangular Prism", ***International Journal of Thermal Sciences,*** 46, 501-505 (2007).

[16] Kalogirou, S.A., "Applications of artificial neural-networks for energy systems", ***Applied Energy,*** 67, 17-35 (2000).

[17] Li, H., Sumner, D., "Vortex shedding from two finite circular cylinders in a staggered configuration", ***Journal of Fluids and Structures***, 25, 479–505, (2009).

[18] Yen, S.C., San, K.C., Chuang, T.H., "Interactions of tandem square cylinders at low Reynolds numbers", ***Experimental Thermal and Fluid Science***, 32, 927–938 (2008).

[19] Fluent 6.1.22., "User's Guide", Fluent Incorporated, Centerra Resource Park, 10 ***Cavendish Court,*** Lebanon, NH 03766, USA, (2001).

[20] Menter, F.R., "Two-equation eddy-viscosity turbulence models for engineering applications", ***AIAA J,*** 32 (8) 1598–605 (1994).

[21] Eiamsa-ard, S. and Promvonge, P., "Numerical study on heat transfer of turbulent channel flow over periodic groove", ***International Communications in Heat and Mass Transfer***, 35: 844-852 (2008).

[22] Lu, B. and Jiang, P., "Experimental and numerical investigation of convection heat transfer in a rectangular channel with angled ribs", ***Experimental Thermal and Fluid Science,*** 30, 513–521, (2006).

[23] Kim, H. and Kim, K., "Shape optimization of three-dimensional channel roughened by angled ribs with RANS analysis of turbulent heat transfer", ***International Journal of Heat and Mass Transfer***, 49, 4013–4022, (2006).

[24] Kamali, R. and Binesh, A.R., "The importance of rib shape effects on the local heat transfer and flow friction characteristics of square ducts with ribbed internal surfaces", ***International Communications in Heat and Mass Transfer***, 35 (8):1032-1040 (2008).

[25] Nasiruddin and Kamran Siddiqui, M.H., "Heat transfer augmentation in a heat exchanger tube using a baffle", ***International Journal of Heat and Fluid Flow,*** 28, 318–328. (2007).

[26] Ozceyhan, V., Gunes, S., Buyukalaca, O. and Altuntop, N., "Heat transfer enhancement in a tube using circular cross sectional rings separated from wall", ***Applied Energy,*** 85 (10):988-1001 (2008).